오일-물-오일 에멀젼막의 Disjoining Pressure에 관한 연구

조 완 구

(엘지 생활건강 화장품연구소)

Disjoining Pressure Isotherms for oil-water-oil Emulsion Films

W-G. Cho[1], B.P. Binks[2] and P.D.I. Fletcher[2]

1. **LG Cosmetics Research Institute 84, Jang-Dong, Yusong-Gu, Taejon 305-343, Korea**
2. **School of Chemistry, University of Hull, Hull HU6 7RX, U.K.**

Abstract

We have used a novel liquid surface forces apparatus(LSFA) to determine the variation of disjoining pressure with film thickness for dodecane-water-dodecane emulsion films. The LSFA allows measurement of film thicknesses in the range 5-100 nm and disjoining pressure from 0-1500 Pa. Disjoining pressure isotherms are given for films stabilised by the nonionic surfactants n-dodecyl pentaoxyethylene glycol ether($C_{12}E_5$) and n-decyl-β-D-glucopyranoside(C_{10}-β-Glu) and the anionic surfactant sodium bis(2-ethylhexyl) sulphosuccinate(AOT) in the presence of added electrolyte. For $C_{12}E_5$ and AOT, the emulsion films are indefinitely stable even for the highest concentration of NaCl tested (136.7 mM) whereas the C_{10}-β-Glu film shows coalescence at this salt concentration. For film thicknesses greater than approximately 20 nm with all three surfactants, the disjoining pressure isotherms are reasonably well described in terms of electrostatic and van der Waals, forces. For the nonionic surfactant emulsion films, the charge properties of the monolayers are qualitatively

similar to those seen for foam films. For AOT emulsion films, the monolayer surface potentials estimated by fitting the isotherms are similar to the values of the zeta potential measured for AOT stabilised emulsion droplets. For thin emulsion films(<20nm) certain systems showed isotherms which suggested the presence of an additional repulsive force with a range of approximately 20nm.

Introduction

This paper concerns measurements of disjoining pressure versus thickness isotherms for thin water films sandwiched between oil phases ("emulsion films") and stabilised by monolayers of either ionic or nonionic surfactants. Although there is a large literature detailing studies of disjoining pressures in water films bounded by vapour phases("foam films") (1-6) using the experimental techniques pioneered by Scheludko (1) and by Mysels and Jones (7), there is only a limited amount of data for emulsion films (8-24). Previous disjoining pressure measurements for emulsion films have been made in two ways. Firstly, film thickness has been determined for a single value of the disjoining pressure (set by the capillary pressure), typically of the order of a few tens of Pa. Secondly, the variation of disjoining pressure with film thickness has been deduced from measurements of the drainage rate where the calculation relies on the assumption of particular hydrodynamic conditions. As discussed, for example, in ref (13), this latter method commonly yields results which do not agree with equilibrium measurements. We have recently developed a novel liquid surface forces apparatus(LSFA) which overcomes these shortcomings and allows the direct determination of the full disjoining pressure isotherm, i.e. the equilibrium film thickness as a function of disjoining pressure over the range 0-1500 Pa (25,26). A feature of the LSFA is that disjoining pressure isotherms may be determined for emulsion films of a few μm radius, i.e. of similar dimensions to the films formed by contact of two emulsion drops in a bulk emulsion. In this paper we report disjoining pressure isotherms for dodecane-water-dodecane emulsion films stabilised by either the anionic surfactant sodium bis(2-ethylhexyl) sulphosuccinate

(AOT) or the nonionic surfactants n-dodecyl pentaoxyethylene glycol ether ($C_{12}E_5$) or n-decyl-β-D- glucopyranoside (C_{10}-β-Glu). Where possible, the results for emulsion films are compared with corresponding data for foam films.

The LSFA in the configuration used to study oil-water-oil films is shown schematically in Figure 1. An oil drop is supported on the tip of a fine glass micropipette which is held initially a few μm below the oil-water interface. The other end of the micropipette is connected to a manometer filled with the same oil. The radius of the oil drop r_o is typically of the order of 10 μm and is controlled by the balance of the Laplace pressure inside the drop and the applied pressure head h according to

$$h\rho g = 2\gamma/r_o \qquad [1]$$

where ρ is the oil density, g is acceleration due to gravity and γ is the oil-water tension. When the oil drop is moved up to the oil-water interface using the piezoelectric translator (piezo 1) a thin Water film is formed between the apex of the drop and the oil-water interface. Under the conditions of this study, the tension of the emulsion film is virtually twice the oil-water tension since the excess film tension arising from the interaction between the two surfactant monolayers is estimated to be of the order of 0.1 mN m^{-1} or less. Hence, the radius of curvature of the film region r_f is double that of the original oil drop(ie. $r_f = 2r_o$). It then follows that the disjoining pressure Π within the film is given by

$$\Pi = h\rho g/2 \qquad [2]$$

The thickness of the emulsion film is determined by analysis of the optical interference pattern collected using the microscope objective lens, video camera and digitising electronics. Full details of the analysis are given in ref.(25). Moving the drop upwards into the oil-water interface (using piezo 1) at constant hydrostatic pressure causes the film radius to increase at constant film thickness. Thus

measurements of the film thickness at different applied hydrostatic pressures yields the variation of Π with film thickness d(the disjoining pressure isotherm).

In addition to determining Π-d isotherms, the total force exerted on the oil drop as it is pushed up to the oil-water interface can also be determined from the extent of vertical deflection of the micropipette. A small mirror is attached to the micropipette as shown in Figure 1. The laser of a reflecto-optical device(ROD) mounted on piezo 2 is focused on the bottom edge of the mirror. The height of the ROD is maintained using piezo 2 with electronic feedback control such that the reflected intensity is approximately half that corresponding to the full reflected intensity measured for the ROD laser focused centrally on the mirror. In this way, the height of the ROD accurately tracks the vertical movement of the mirror and thus records the vertical deflection of the mirror resulting from a force between the oil drop and the oil-water interface. The force is calculated from the measured deflection and the(separately determined) force constant of the micropipette. As described in refs.(25,26), the variation of the force and the radius of the film as a function of the vertical micropipette position can be quantitatively accounted for in terms of independently measured parameters for each system and provide convincing confirmation of the validity of the technique. Full experimental details of the LSFA and the theoretical analysis are given in refs.(25,26).

In this paper we present disjoining pressure isotherms for dodecane-water-dodecane emulsion films stabilised by the anionic surfactant AOT and the nonionic surfactants $C_{12}E_5$ and C_{10}-β-Glu for different concentrations of NaCl in the aqueous phase. Where possible, the results for emulsion films are compared with those for the corresponding foam films. The measured disjoining pressure isotherms are compared with isotherms calculated assuming that the disjoining pressures are dominated by contributions due to electrostatic repulsion and van der Waals forces.

Experimental

n-Dodecane (>99%, Aldrich) was passed twice over an alumina column prior to use to remove trace, polar impurities. The anionic surfactant AOT was supplied by Sigma and used without further purification. The nonionic surfactants $C_{12}E_5$ (Nikko, > 99%) and C_{10}-β-Glu(Sigma-Aldrich) were used as supplied. Water was purified by reverse osmosis and passed through a Milli-Q reagent water system. NaCl (AR grade) was from Prolabo.

Interfacial tension measurements were made using either a Kruss K10 du Nouy ring tensiometer or a Kruss Site 04 spinning drop tensiometer using procedures described previously (27).

Disjoining pressure measurements were made using the LSFA as described in refs.(25,26). The measurements were made by stopping the micropipette movement and recording the force, film radius and thickness at fixed micropipette position. Steady values were achieved within a minute or so after stopping the micropipette movement and thus the results refer to equilibrium values and are not perturbed by effects associated with hydrodynamic forces or film drainage. No difference was observed between values obtained by increasing or decreasing the hydrostatic pressure. As described in ref (25), the maximum value of Π that can be measured using the LSFA is determined by the oil-water tension and the inner radius of the micropipette tip. In order to achieve the widest possible range of disjoining pressures, several runs were made for each system using micropipettes of different radius. All experiments were carried out at room temperature, $20 \pm 1°C$.

Results and Discussion

Dodecane-aqueous NaCl-dodecane films stabilised by $C_{12}E_5$

Measurements were made for aqueous solutions containing 0.02 mM $C_{12}E_5$(equal to approximately cmc/3) and different concentrations of NaCl. $C_{12}E_5$ distributes between alkanes and water and the equilibrium distribution coefficient (i.e. $C_{12}E_{5dodecane}[C_{12}E_5]_{water}$ with the concentrations entered in units of M) is estimated to be 210 at 20°C(28,29) and was taken to be independent of [NaCl] over the salt concentration range studied here. In order to avoid non-equilibrium effects associated with transfer of surfactant from the aqueous phase to the dodecane, the estimated equilibrium concentration of $C_{12}E_5$ (4.2 mM) was added to the dodecane. Oil-water tensions and cmc values for the different surfactant systems investigated are summarised in table 1.

For all the different system, it was checked that the variation of force and film radius with micropipette position(pipx) was correctly described by the equations given in ref.(25). Figures 2 and 3 shows an illustrative example of a $C_{12}E_5$ system where it can be seen that the experimental data is well described by the calculated curves using the independently measured parameters listed in the figure legends.

Figure 4 shows isotherms determined from the variation in film thickness with applied hydrostatic pressure(equal to twice the disjoining pressure) for $C_{12}E_5$ films with different NaCl concentrations. It can be seen that the disjoining pressure isotherms are repulsive(i.e. Π is positive) and very sensitive to the salt concentration. This suggests that the forces are dominated by long range electrostatic repulsive forces.

In general, the total film disjoining pressure Π is generally taken to be the sum of contributions arising from repulsive electrostatic forces (Π_{el}), attractive van der Waals forces(Π_{vdw}) and repulsive short range forces arising from hydration, monolayer undulations and other sources (30). As a first stage in attempting to account for the measured isotherms, we compare the experimental data with isotherms calculated on the assumption that $\Pi = \Pi_{el} + \Pi_{vdw}$. For surfaces of equal charge density in the presence of a 1:1 electrolyte, Π_{el} is given to a reasonable approximation for the relatively thick films considered here by the so-called "weak-overlap" approximation

(30).

$$\Pi_{el} = 64ckTtan\ h^2\left(\frac{e\Psi_0}{4kT}\right)\exp(-kd) \qquad [3]$$

where c is the ionic concentration, k is the Boltzmann constant, T is the temperature, e is the electronic charge, Ψ_0 is the surface potential, d is the film separation and κ is the reciprocal Debye length defined by

$$\kappa^{-1} = \sqrt{\frac{\varepsilon\varepsilon_0 kT}{2e^2 c}} \qquad [4]$$

where ε is the relative permittivity the film liquid and ε_o is the permittivity of free space. The charge density at the surface σ_o can be related to the surface potential by using the Grahame equation.

$$\sigma_0 = \sqrt{8\varepsilon\varepsilon_0 kTc}\sinh(e\Psi_0/2kT) \qquad [5]$$

It was checked that, for the range of film thicknesses and disjoining pressures encountered in the present study, exact calculations of Π_{el}, made using the algorithm described by Chan et al.(31) with assumption of either constant surface charge or constant surface potential, yielded results identical to those given by equation 3. For the calculation of the attractive van der Waals' component we use the usual expression for non-retarded forces (30),

$$\Pi_{vdw} = -A/6\,\pi d^3 \qquad [6]$$

where A is the Hamaker constant which has the value of approximately 0.5×10^{-20} J for dodecane-water-dodecane films (30). We note here that the attractive van der Waals' forces are likely to be over-estimated for separations greater than approximately 5 nm where retardation effects become significant (30).

Calculated curves for Π versus d(solid lines) are compared with experiment in

Figure 4. Using only the surface potential as an adjustable parameter, reasonable fits to the isotherms are obtained For NaCl concentrations of 8.55 and 51.3 mM, a slight deviation between theory and experiment is seen in the region of high thickness and low Π. Although the effect is of a similar magnitude to the experimental uncertainties, the measured isotherms appear to decay less rapidly with separation than predicted. A plausible explanation for this is that the van der Waals, attraction is over-estimated in this regime due to neglect of retardation effects.

Values of the surface potential obtained from such fits, together with derived values of the surface charge density are shown in Figure 5 as a function of the salt concentration. The origins of the charge properties in surface films of nonionic surfactants has been the subject of much debate and many experimental studies for foam film surfaces. Many aspects of this problem are discussed in a paper by Manev and pugh (32) which describes results for foam films stabilised by $C_{12}E_5$ as a function of surfactant concentration, pH and KCl concentration. For the foam films, the limiting surface potential at low surfactant concentration is approximately -45 mV(similar to that for the pure air-water surface at the pH of the experiments) and decreases in magnitude to approximately -10 mV as the $C_{12}E_5$ concentration is increased to values around the cmc. The potential is vanishingly small for pH $<$ 3 and becomes increasingly negative to reach an asymptotic value for pH above about 7. Manev and Pugh observe that the surface potentials for 10^{-4} M KCl are generally a few mV larger than for 10^{-3} KCl. Using some interpolation of the data sets for the foam and emulsion films, some comparison of the values can be made. The surface potentials for the emulsion films(Figure 5) with$[C_{12}E_5]$ = 0.02 mM, pH =5.5 and [NaCl] =10^{-3} or 10^{-4} M are approximately -82 and -45 mV respectively. These values are significantly larger than for the foam films under the same conditions (except that KCl is added instead of NaCl)where the values are approximately -33 mV for both salt concentrations. Since the surface potential appears to arise from the properties of the bare fluid-fluid interface, it is of interest to compare the zeta potentials of the pure air-water and dodecane-water surfaces. For pH 6, the value for dodecane-water is -58 mV (33), significantly higher than the value for the air-water

surface of -23 mV (34). Thus, the higher potentials seen for the emulsion films may have their origin in the different ion adsorption properties of the bare interfaces. It is noteworthy that the zeta potential of the bare xylene-water interface decreases in magnitude with increasing [NaCl] (33) as seen here for the $C_{12}E_5$ emulsion films.

C_{10}-β Glu stabilised films

Because of increasing environmental concerns, there is current interest in seeking alternatives to nonionic surfactants based on polyoxyethylene. Possible candidates showing improved biodegradability are surfactants containing sugar groups as the hydrophilic moiety, However, sugar surfactants commonly show differences in their properties as emulsifiers and foam stabilisers when compared with surfactants based on polyoxyethylene (35,36). Since the different emulsification properties may arise, at least in part, from the different colloidal forces between monolayers of the two types of surfactant, we have investigated disjoining pressure isotherms for emulsion films stabilised by C_{10}-β Glu.

The emulsion films were stabilised by a concentration of C_{10}-β Glu equal to 0.5mM which corresponds to approximately cmc/4 and an oil-water interfacial tension of 13.2 mN m^{-1} (Table 1). We attempted to measure disjoining pressures for [NaCl] = 136.7 mM. However, unlike the case of $C_{12}E_5$ for which the emulsion films at this high salt concentration were observed to be stable indefinitely, films stabilised by C_{10}-β Glu with 136.7 mM NaCl showed coalescence with the oil-water interface within a minute or so after contact between the oil drop and interface. This difference in behaviour may be related to the higher sensitivity of the cloud points of sugar surfactants to the addition of salt as compared with alkyl ethoxylate surfactants(35).

Figure 6 shows the disjoining pressure isotherms measured for various concentrations of NaCl. For the three lowest salt concentrations corresponding to the thickest films, the curves were reasonably well described using calculated curves corresponding to the surface potentials listed in Table 2. The surface potentials

estimated from the fits are similar to those for $C_{12}E_5$ films at the same salt concentrations. The curve for 8.55 mM NaCl was found to be irreproducible with the data for one run(Π values in the range 500-1000 Pa) showing anomalously low thicknesses. This result may indicate that the thick films are metastable and may undergo a transition to a thin film. For 51.3 mM NaCl, the measured thicknesses for two independent runs lay on a consistent curve ;however, the measured thicknesses were significantly larger than could be accounted for by calculations of Π_{el} and Π_{vdw}. This is shown by the dashed curve in Figure 6 which corresponds to the maximum possible repulsive theoretical disjoining pressure(calculated using Ψo = 5V(this physically unrealistic large value of the surface potential corresponds to maximum possible electrostatic repulsion) and A =0). This result suggests the presence of an additional repulsive force with a range of approximately 20 nm may be operating across these films. One possible explanation is that the additional repulsion arises from ionic volume exclusion effects which act to increase the electrostatic repulsion over that calculated using equation 3(37). We emphasise here that this conclusion is rather tentative and further investigation of a wider range of thin films is required to confirm this observation.

Studies of foam films stabilised by alkyl glucosides(mainly octyl-β-glucoside) in the presence of added KBr are described in refs.(38-40). As seen for the case of $C_{12}E_5$, monolayer surface potentials for the foam films are generally smaller than for the emulsion films under similar conditions of salt and surfactant concentration relative to the respective cmc values.

AOT stabilised films

The behaviour of the nonionic systems is compared with that of monolayers stabilised by the anionic surfactant AOT. The disjoining pressure curves shown in Figure 7 fall into two series as shown in Table 1. Firstly, the AOT concentration was increased from below the cmc to above the cmc at zero salt concentration. For the second series containing added NaCl, the AOT was adjusted so as the keep the

oil-water tension constant at 18 mN m^{-1}. For all the salt and AOT concentrations tested, the emulsion films were found to be indefinitely stable.

The experimental isotherms in Figure 7 are compared with curves calculated using the assumption that only electrostatic and van der Waals' forces are operating. Using a value of the Hamaker constant A =0.5 x 10^{-20} J, fitting of the curves yielded the surface charge parameters listed in Table 3. The surface potential remains approximately constant at 80-90 mV (negative). Similar values have been measured for the zeta potential of heptane -in-water emulsion droplets for a range of NaCl concentrations(41). The calculated curves show reasonable agreement with experiment except for the case of 51.3 mM NaCl where the calculated curve appears to show insufficient repulsion to account for the results. It is not possible to increase the surface potential to obtain a match with the data for this case without producing physically unreal large values of the surface charge density, Thus, as for the case of C_{10}-β-Glu, the data suggests the presence of an additional repulsive force with a range of approximately 20 nm.

Conclusions

We have determined disjoining pressure isotherms for dodecane emulsion films stabilised by $C_{10}E_5$, C_{10}-β-Glu and AOT as functions of the aqueous phase concentration of salt. For films thicknesses greater than approximately 20 nm, the isotherms are well described using standard equations for electrostatic repulsion and van der Waals' attraction. For films of thickness less than 20 nm, we have observed a number of cases where the experimental isotherms suggest the presence of an additional repulsive force.

References

1. Scheludko, A., *Adv. Colloid Interface Sci.*, 1967, *1*, 391.
2. Clunie. J.S., Goodman, J.F. and Ingham B.T., in "Surface & Colloid Science, Ed. Matijevic, E., Vol. 3, Wiley, New York. 1971.
3. Sonntag, H. and Strenge, K., "Coagulation and Stability of Disperse Systems", (translated by R. Kondor), Halsted Press, New York, 1972.
4. Aveyard, R. and Vincent, B., *Prog. in Surface Sci.*, 1977, *8*, 59.
5. *"Thin Liquid Films. Fundamentals and Applications"*, Ed. Ivanov, I.B., Marcel Dekker, Surfactant Science Series, Vol. 29, New York, 1988.
6. Exerowa, D., Kashchiev, D. and Platikanov, D., *Adv. Colloid Interface Sci.*, 1992, *40*, 201.
7. Mysels, K.J. and Jones, M.N., *Disc. of the Faraday Soc.*, 1966, No. 42, 42.
8. Van den Tempel, M., *J. Colloid Sci.*, 1958, *13*, 125.
9. Sonntag, H., Netzel, J. and Klare, H., *Kolloid Zeit. and Zeit Polymere*, 1966, *211*, 121.
10. Netzel, J. and Sonntag, H., *Abh. Dtsch. Akad Wiss. Ki. Chem., Geol. Biol.*, 1966, *6A*, 589.
11. Platikanov, D. and Manev, E., Proceedings of the IVth International congress on Surface Active Substances, Volume II, Physics and Physical Chemistry of Surface Active Substances, Ed. Overbeek, J.Th.G., Gordon and Breach, London, 1967, p.1189.
12. Sonntag, H., Netzel, J. and Unterberger, B., *Spec. Discuss. Faraday Soc.*, 1970, *1*, 57
13. Herringion, T.M., Midmore, B.R. and Sahi S.S., *J. Chem. Soc. Faraday Trans. 1*, 1982, *78*, 2711.
14. Manev, E.D., Sazdanova, S.V. and Wasan, D.T., *J. Dispersion Sci. Technol.*, 1984, *5*, 111.
15. Fisher, L.R. and Parker, N.S., *Faraday Discuss. Chem. Soc.*, 1986, *81*, 249.
16. Ivanov, I .B., Chakarova, SV.K. and Dimitrova B.I., *Colloids and Surfaces*, 1987, *22*, 311.

17. Muller, H.J., Balinov, B.B. and Exerowa, D.R., *Colloid Polym. Sci.*, 1988, *266*, 921.

18. Fisher, L.R., Mitchell, E.E. and Parker, N.S., *J. Colloid Interface Sci.*, 1989, *128*, 35.

19. Velev, O.D., Gurkov, T.D., and Borwankar, *J. Colloid Interface Sci.*, 1993, *159*, 497.

20. Velev, O.D., Nikolov, A.D., Denkov, N.D., Doxastakis, G., Kiosseoglu, V. and Stalidis, G., *Food Hydrocolloids*, 1993, *7*, 55.

21. Velev, O.D., Gurkov, T.D., Chakarova, Sv.K., Dimitrova, B.I., Ivanov, I.B. and Borwankar, R.P., *Colloids and Surfaces A:Physicochemical and Engin. Aspects*, 1994, *83*, 43.

22. Velev, O.D., Gurkov, T.D., Ivanov, I.B., and Borwankar, R.P., *Phys. Rev. Letts.*, 1995, *75*, 264.

23. Velev, O.D., Constantinides, G.N, Avraam D.G., Payatakes, A.C. and Borwankar, R.P., *J. Colloid Interface Sci.*, 1995, *175*, 68.

24. Koczo, K., Nikolov, A.D., Wasan, D.T., Borwankar, R.P. and Gonsalves, A., *J. Colloid Interface Sci.*, 1996, *178*, 694.

25. Aveyard, R., Binks, B.P., Cho, W-G., Fisher, L.R., Fletcher, P.D.I. and Klinkhammer, F., *Langmuir*, 1996, *12*, 6561.

26. Cho, W-G. and Fletcher, P.D.I., J. Chem. Soc. Faraday Trans. 1997, 931, 1389.

27. Aveyard, R., Binks, B.P., Clark, S. and Mead, J., *J. Chem. Soc. Faraday Trans. 1*, 1986, *82*, 125.

28. Aveyard, R., Binks, B.P., Clark, S and Fletcher, P.D.I., *Chem. Soc. Faraday Trans.*, 1990, *86*, 3111.

29. Aveyard, R., Binks, B.P., Fletcher, P.D.I. and Ye, X., *J. Chem. Tech. Biotechnol*, 1992, *54*, 231.

30. Israelachvili, J.N., *"Intermolecular and Surface Forces"*, 2nd Ed., Academic press, London, 1992.

31. Chan, D.Y.C, Pashley, R.M. and White, L.R., *J. Colloid Interface Sci.*, 1980, *77*, 283.

32. Manev, E.D. and Pugh, R.J., *Langmuir*, 1991, *7*, 2253.

33. Marinova, K.G., Alargova, R.G., Denkov, N.D., Velev, O.D., Petsev, D.N., Ivanov, I.B. and Borwankar, R.P., *Langmuir*, 1996, *12*, 2045.
34. McShea, J.A. and Callaghan, I.C., *Colloid Polymer Sci.*, 1983, *261*, 757.
35. *"Alkyl Polyglycosides"*, Eds. Hill, K., von Rybinski, W. and Stoll, G., VCH, Weinheim, 1997.
36. Aveyard, R. Binks, B.P., Chen, J. and Fletcher, P.D.I., University of Hull unpublished results.
37. Paunov, V.N, Dimova, R.I., Kialchevsky, P.A., Broze, G. and Mehreteab, A., *J. Colloid Interface Sci.*, 1996, *182*, 239.
38. Waltermo, A., Manev, E., Pugh, R. and Claesson P., *J. Dispersion Sci. Technol.*, 1994, *15*, 273.
39. Begeron, V., Waltermo, A. and Claesson, P.M., *Langmuir*, 1996, *12*, 1336.
40. Waltermo, A., Claesson, P.M., Simonsson, S., Manev, E., Johansson, I. and Bergeron, V., *Langmuir*, 1996, *12*, 5271.
41. Aveyard, R., Binks, B.P., Cho, W-G., Fletcher, P.D.I. and Petsev, D.N., University of Hulll unpublished results.

Table 1. Summary of dodecane-water interfacial tension and cmc values (at zero added NaCl) for the surfactant plus NaCl solutions investigated.

surfactant	[surfactant]/mM	[NaCl]/mM	γ/mN^{-1}
$C_{12}E_5$	0.02	0	6.46
cmc = 0.064 mM	0.02	0.1	6.45
	0.02	0.7	6.46
	0.02	8.55	6.49
	0.02	51.3	6.66
	0.02	136.7	6.89
C_{10}-β-Glu	0.5	0	13.17
cmc = 2.1 mM	0.5	0.1	13.17
	0.5	0.7	13.19
	0.5	8.55	13.15
	0.5	51.3	-
AOT	0.3	0	18.0
cmc = 2.3 mM	1.0	0	8.1
	3.0	0	3.0
	0.11	8.55	18.0
	0.031	51.3	18.0
	0.0135	136.7	18.0

Table 2. Surface potentials and charge densities for C_{10}-β-Glu monolayers at the dodecane-water interface at 20°C. The aqueous phase concentration of C_{10}-β-Glu was 0.5 mM. The salt concentration corresponding to no added salt (marked a) was estimated by treating it as an adjustable parameter. As detailed in the text, the fit to the experimental data for the two highest salt concentrations (superscripted b)is poor and the values of ψ_0 and σ_0 are indeterminate.

[NaCl] /mM	k^{-1}/nm	Iψ_0I/mV	σ_0/electronic charges nm^{-}
0.08[a]	34.1	105	0.025
0.1	30.5	77	0.016
0.7	11.5	77	0.042
8.55[b]	3.3	(120)[b]	(0.36)[b]
51.3[b]	1.35	(100)[b]	(0.58)[b]

Table 3. Surface potentials and charge densities for AOT monolayers at the dodecane-water interface at 20°C.

[AOT]/mM	[NaCl]/mM	κ^{-1}/nm	$\lvert\psi_0\rvert$/mV	σ_0/electronic charges nm^{-2}
0.3	0	17.6	90	0.036
1.0	0	9.6	85	0.059
3.0	0	5.6	90	0.114
0.11	8.55	3.3	80	0.16
0.031	51.3	1.35	80	0.38
0.0135	136.7	0.83	80	0.62

Figure Legends

Figure 1. Schematic diagram of the liquid surface forces apparatus (LSFA). The lower diagrams show the isolated micropipette with mirror extension arm and mirror attached and a close up view of the tip of the pipette supporting an oil drop close to the oil-water interface.

Figure 2. Variation of film radius r with micropipette position pipx for 0.02 mM $C_{12}E_5$ with 136.7 mM NaCl. The vertical position of the micropipette tip pipx = 0 is taken to be point at which the apex of the oil drop first contacts the oil-water interface. The hydrostatic pressure was 954 Pa and the inner radius and force constant of the micropipette were 10.5 μm and 0.0193 N m^{-1} respectively, The solid line is calculated using only independently measured parameters as described in ref.(25).

Figure 3. Variation of force with pipx for the same system and conditions as in Figure 2. The solid line is the calculated curve.

Figure 4. Disjoining pressure isotherms for oil-water-oil emulsion films stabilised by 0.02 mM $C_{12}E_5$ for [NaCl] equal to 0.1(open circles), 0.7(filled circles), 8.55(open triangles), 51.3(filled triangles) and 136.7 mM(open squares). The solid lines are calculated as described in the text.

Figure 5. Variation of surface potential (upper plot) and surface charge density (lower plot) for emulsion films stabilised by 0.02 mM $C_{12}E_5$

Figure 6. Disjoining pressure isotherms for oil-water-oil emulsion films stabilised by 0.5 mM C_{10}-β-Glu for [NaCl] equal to 0(open circles, concentration of monovalent electrolyte estimated to be 0.08 mM), 0.1(filled circles), 0.7(open triangles), 8.55(filled triangles) and 51.3 mM (open squares). The solid lines are calculated as described in the text using the values of

surface potential listed in Table 2. The dashed line indicates an alternative calculated curve for 51.3 mM NaCl with ψ_0 = 5 V and Hamaker constant equal to zero.

Figure 7. Disjoining pressure isotherms for oil-water-oil emulsion films stabilised by AOT. The symbols refer to the following aqueous phase concentrations of AOT and NaCl (units mM) : 0.3 and 0(open circles), 1.0 and 0(filled circles), 3.0 and 0(open triangles), 0.11 and 8.55(filled triangles), 0.031 and 51.3(open squares) and 0.0135 and 136.7(filled squares). The solid lines are calculated as described in the text using the values of surface potential listed in Table 3.

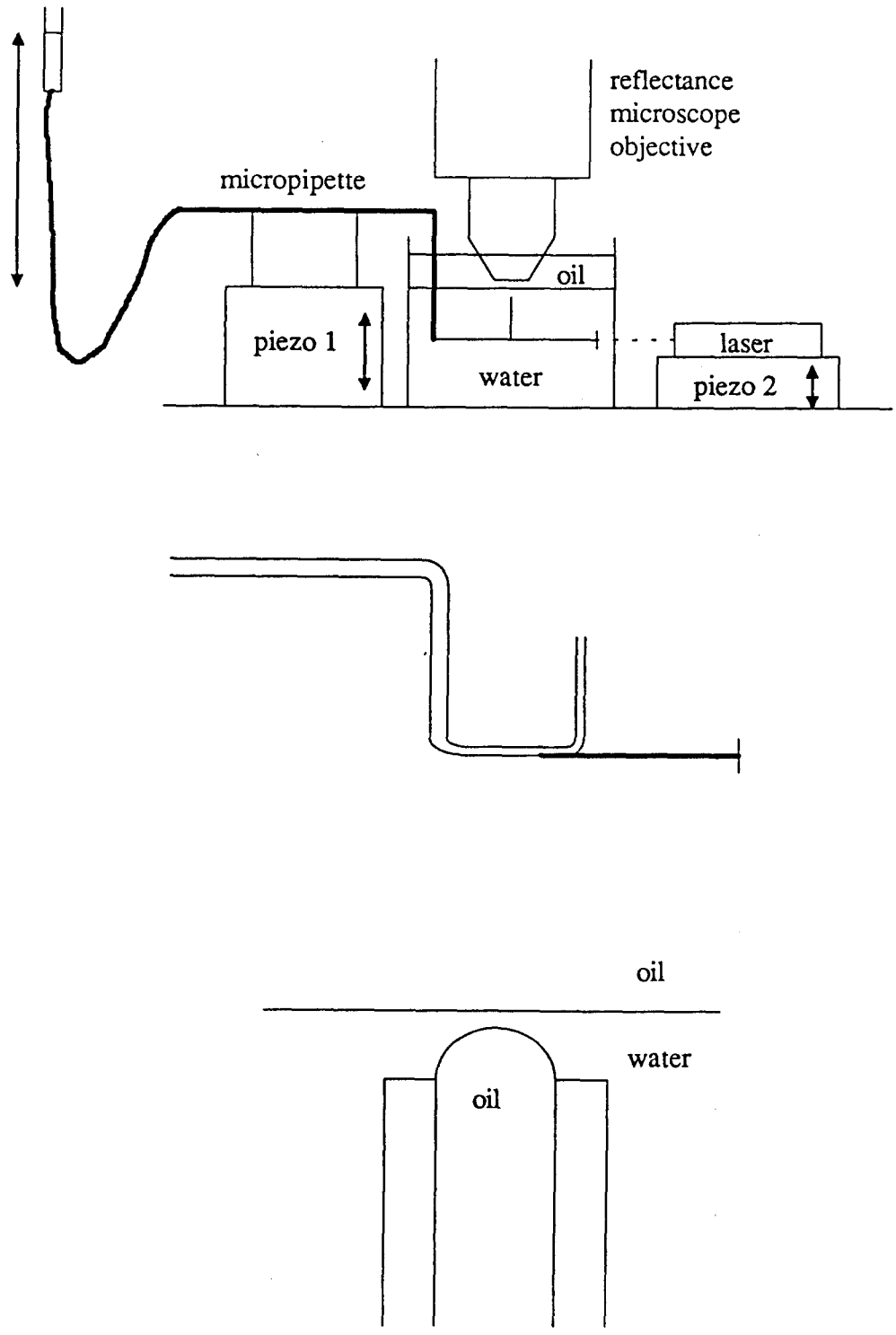
reflectance
microscope
objective
micropipette
oil
piezo 1
water
laser
piezo 2
oil
water
oil

Figure 1.

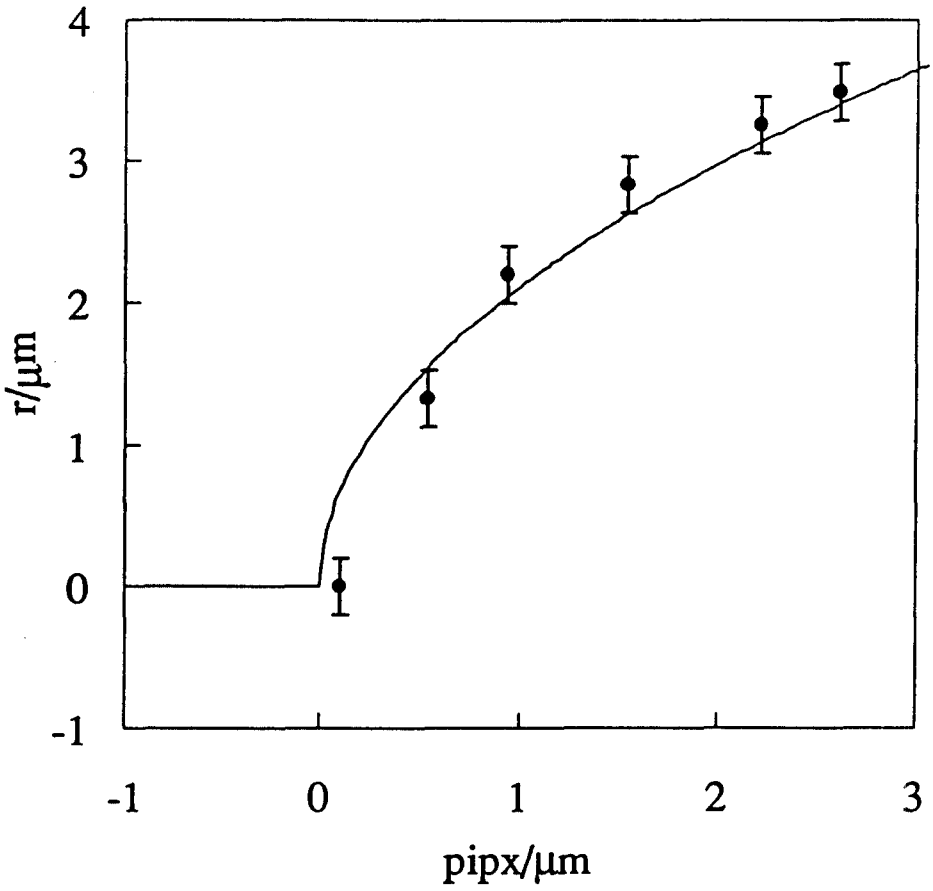

Figure 2.

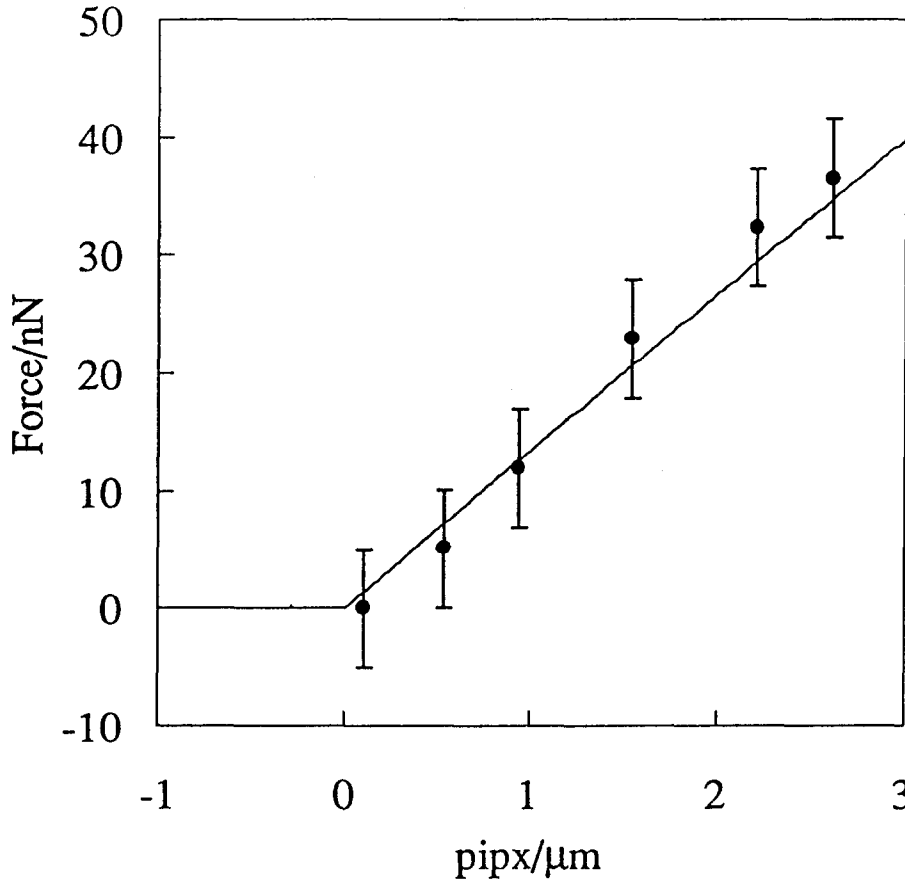

Figure 3.

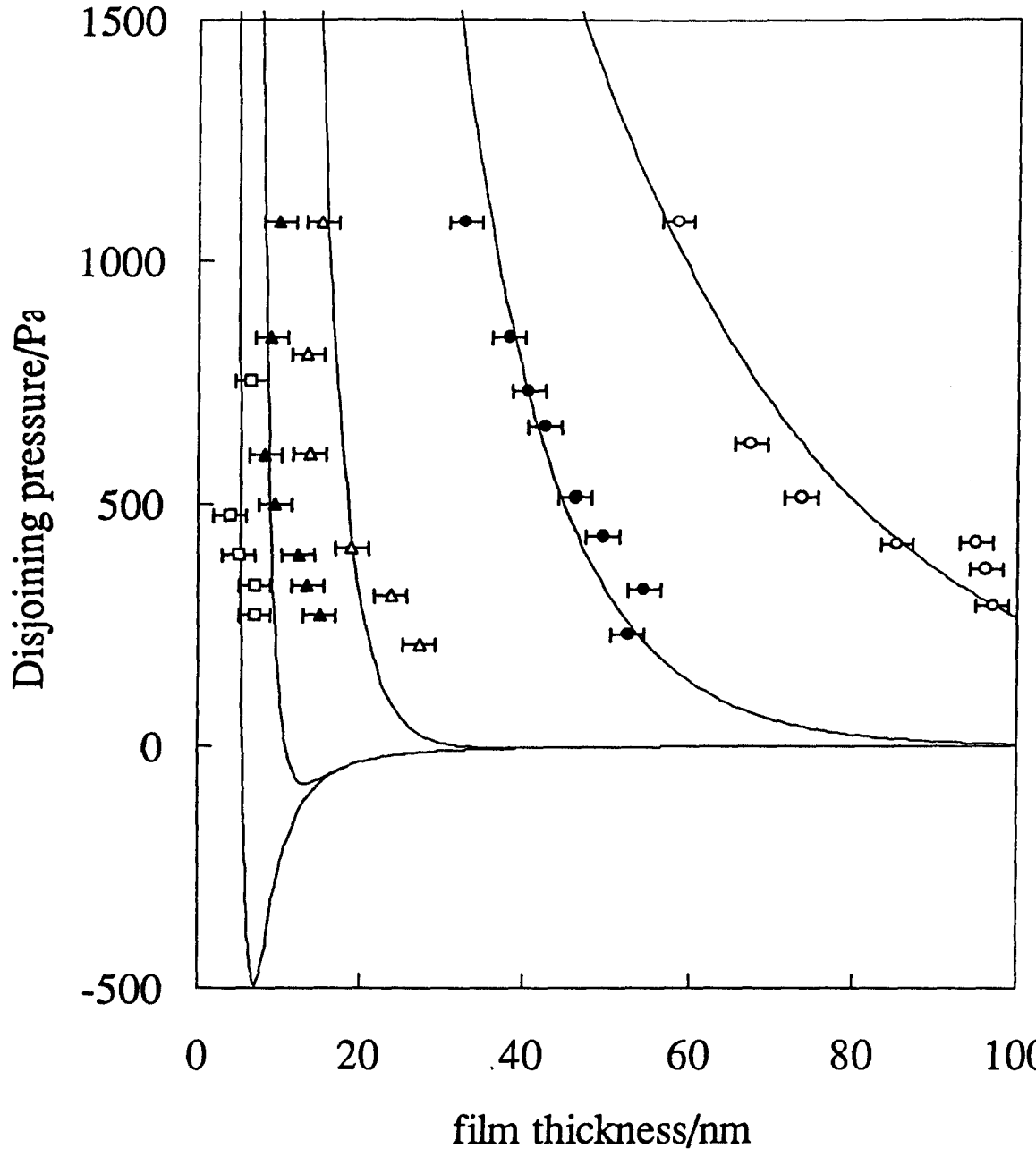
1500
1000
500
0
-500
Disjoining pressure/Pa
0
20
40
60
80
100
film thickness/nm

Figure 4.

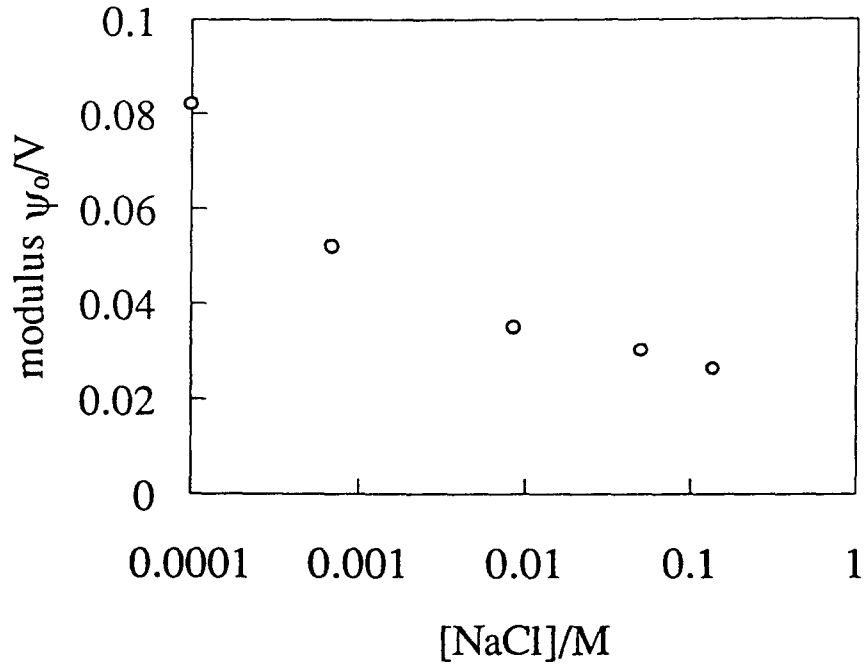
0.1
0.08
0.06
0.04
0.02
0
modulus ψo/V
0.0001
0.001
0.01
0.1
1
[NaCl]/M

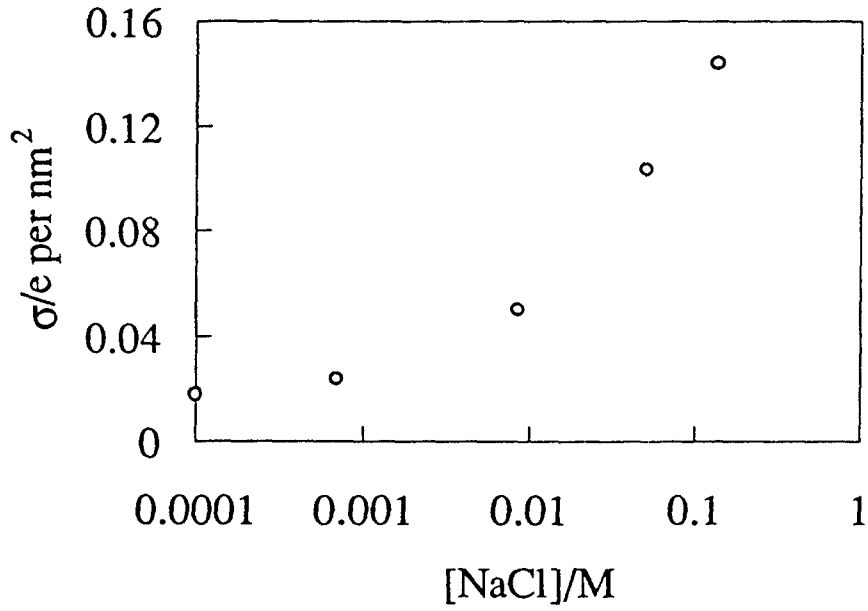
0.16
0.12
0.08
0.04
0
σ/e per nm2
0.0001
0.001
0.01
0.1
1
[NaCl]/M

Figure 5.

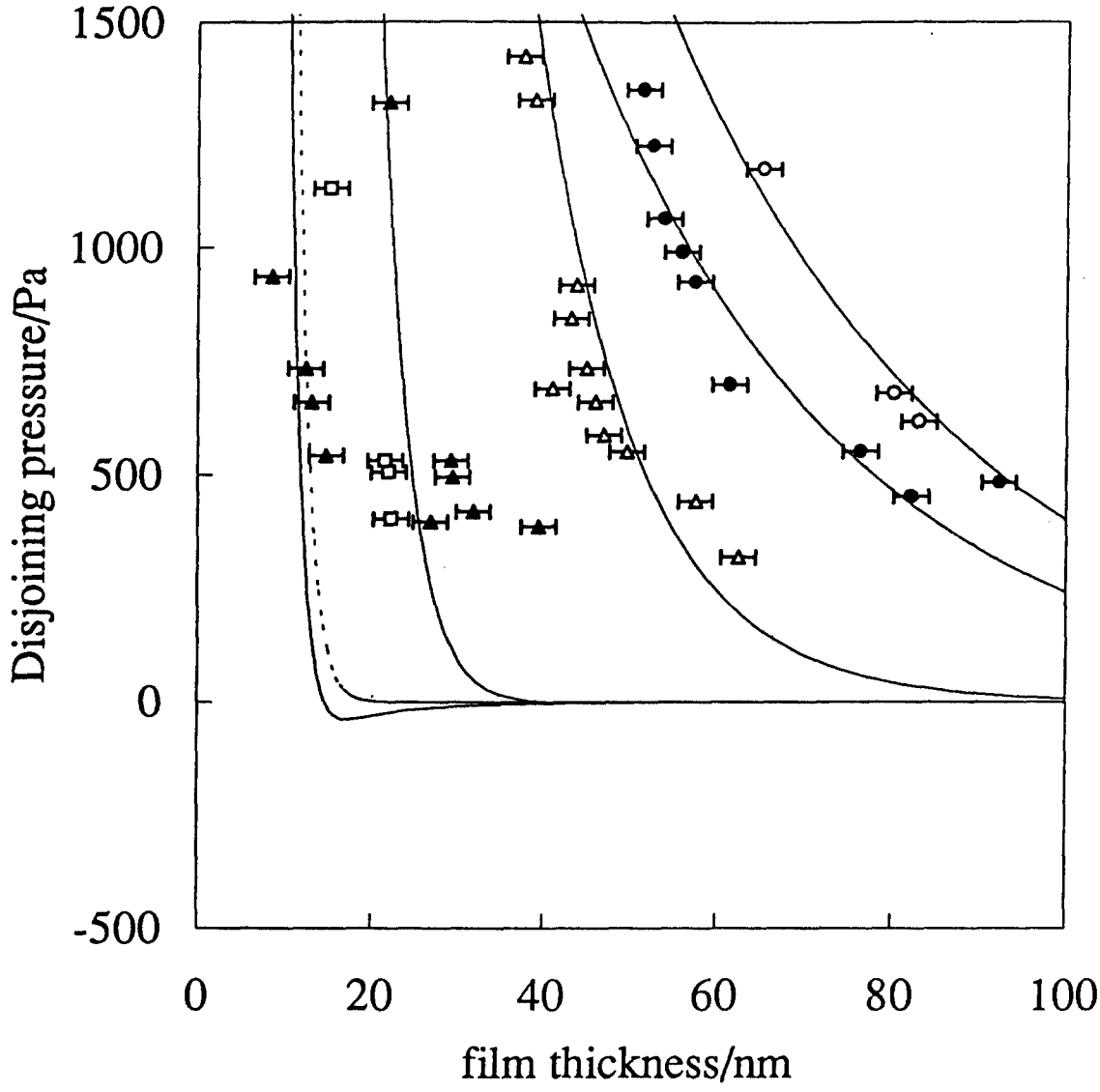
1500
1000
500
0
-500
Disjoining pressure/Pa
0
20
40
60
80
100
film thickness/nm

Figure 6.

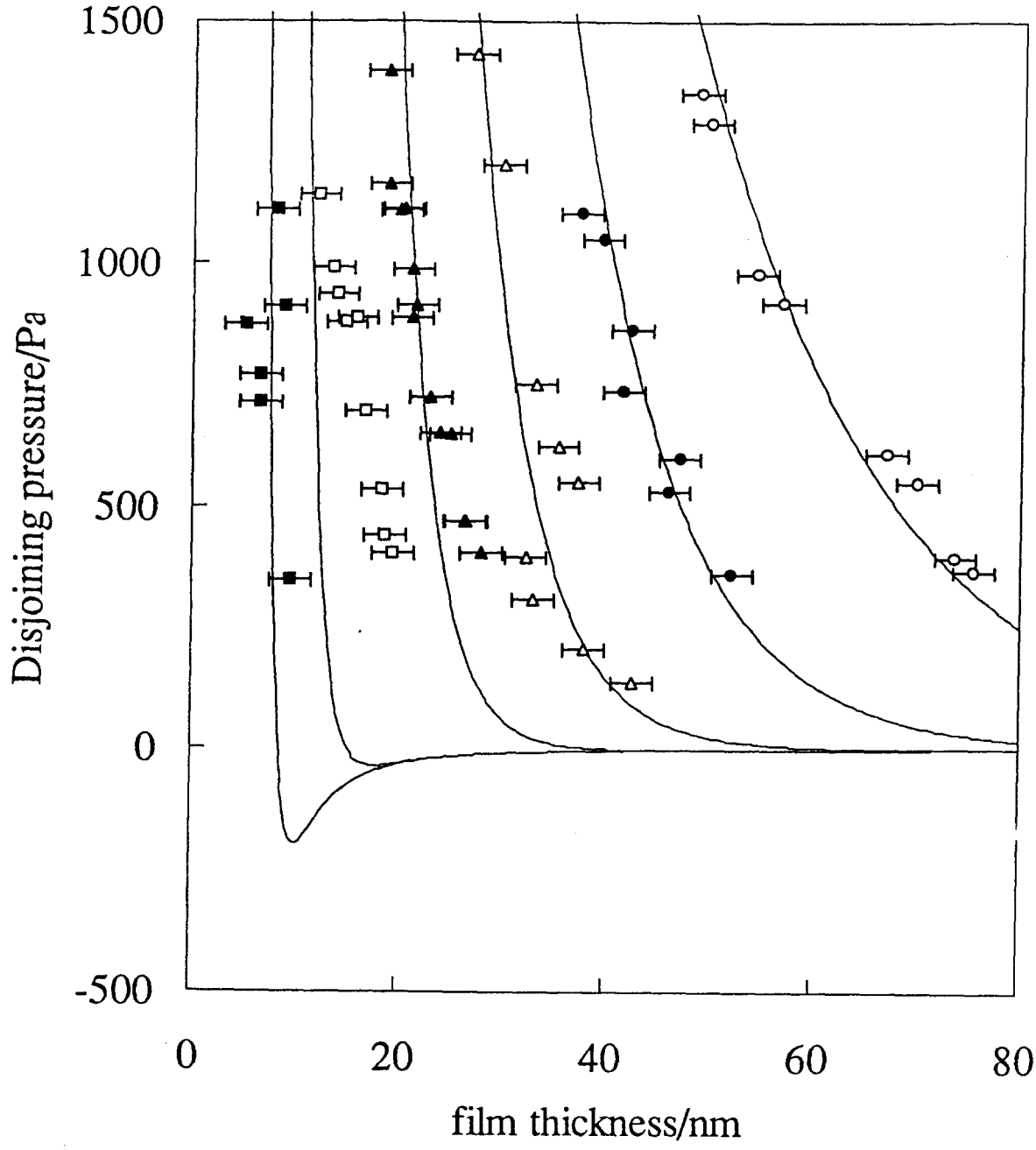
1500
1000
500
0
-500
Disjoining pressure/Pa
0
20
40
60
80
film thickness/nm

Figure 7.